PERGAMON

International Journal of Solids and Structures 37 (2000) 4377–4401

INTERNATIONAL JOURNAL OF SOLIDS and STRUCTURES

www.elsevier.com/locate/ijsolstr

Three-dimensional transient piezothermoelasticity in functionally graded rectangular plate bonded to a piezoelectric plate

Yoshihiro Ootao*, Yoshinobu Tanigawa

Department of Mechanical Systems Engineering, Osaka Prefecture University, 1-1 Gakuen-cho, Sakai, 599-8531, Japan

Received 21 August 1998; in revised form 9 September 1999

Abstract

In this study, the theoretical analysis of a three-dimensional transient piezothermoelasticity problem is developed for a functionally graded rectangular plate bonded to a piezoelectric plate due to partial heat supply. In this analysis, temperature distribution has a dependence on time, while the inertia term is ignored. Assuming the functionally graded rectangular plate has nonhomogeneous thermal and mechanical material properties in the thickness direction, the three-dimensional temperature in a transient state and three-dimensional transient thermal stresses of a simple supported plate for functionally graded material are analyzed by introducing the theory of laminated composites as a theoretical approximation. By using the solution for a functionally graded plate and the exact solution for piezoelectric plate of crystal class mm2, the theoretical analysis of three-dimensional transient piezothermoelasticity is developed for a simply supported combined plate. As an example, numerical calculations are carried out for a functionally graded rectangular plate made of zirconium oxide and titanium alloy, bonded to a piezoelectric plate of a cadmium selenide solid. Some numerical results for the temperature change, the displacement, the stress, electric potential, and electric displacement distributions in a transient state are shown in figures.

Keywords: Elasticity; Thermal stress; Functionally graded material; Piezoelectricity; Rectangular plate; Three-dimensional problem; Transient state

1. Introduction

In recent years, nonhomogeneous materials such as functionally graded materials (FGM) have been

* Corresponding author. Tel.: +81-722-54-9210; fax: +81-722-54-9904.
E-mail address: ootao@center.osakafu-u.ac.jp (Y. Ootao).

0020-7683/00/$ - see front matter
PII: S0020-7683(99)00257-7

developed as new material that is adaptable for a super-high-temperature environment. FGM are made of a mixture with arbitrary composition of engineering ceramics and light metal, and the volume fraction of each material is changed gradually. Thus, it is possible to change the thermal stress distribution by the control of the volume fraction of these two materials. And it is well-known that thermal stress distributions in a transient state can show large values compared with the one in a steady state. Therefore, the transient thermal stress problems for these nonhomogeneous materials become important and there are several analytical studies concerned with these problems. One-dimensional transient thermal stress problems for nonhomogeneous plate were reported (Sugano, 1987; Obata and Noda, 1993; Tanigawa et al., 1996). As a study of three-dimensional problem, we recently analyzed the three-dimensional transient thermal stress problems for a nonhomogeneous hollow circular cylinder (Ootao et al., 1995a) and nonhomogeneous hollow sphere (Ootao and Tanigawa, 1995b) by introducing the theory of laminated composites as an approximation.

On the other hand, piezoelectric materials have coupled effects between the elastic fields and the electric field, and have become of major interest lately as the functional materials such as actuators or sensors (Rao and Sunar, 1994). It is possible to make a system of intelligent composite materials by combining these piezoelectric materials with structural materials. As a result, several analytical studies concerned with piezothermoelasticity of intelligent composite materials were reported. For example, Tauchert (1992) and Noda and Kimura (1998) treated the response of a thin fiber-reinforced composite plate with a piezoelectric plate. Ashida et al. (1996) treated an inverse piezothermoelasticity problem of an isotropic plate with a piezoelectric plate. Ashida et al. (1997) and Choi et al. (1997) treated the control of thermally induced elastic displacement of an isotropic plate with a piezoelectric plate. The reports concerned with intelligent FGM are few. So far as we know, Qiu et al. (1994) treated a piezothermoelasticity problem of FGM beam with a piezoelectric layer. However this problem is analyzed using finite element method.

In the present paper, we analyzed the three-dimensional piezothermoelasticity in a functionally graded rectangular plate bonded to a piezoelectric plate of crystal class mm2 due to partial heat supply in the transient state.

2. Analysis

We now consider the functionally graded rectangular plate to which a piezoelectric plate of crystal class mm2 is perfectly bonded. We assume that the functionally graded plate has nonhomogeneous thermal and mechanical material properties in the thickness direction and the combined rectangular plate is simply supported at all edges. As an analysis of FGM plate, the heat conduction problem and the associated thermoelastic behavior are developed introducing the theory of laminated composites as a theoretical approximation. In this analysis, temperature distribution has a dependence on time, while the inertia term is ignored.

3. Heat conduction problem

We consider a functionally graded rectangular plate bonded to a piezoelectric plate as shown in Fig. 1. The thickness of the functionally graded plate and piezoelectric plate are represented by B and b, respectively. The lengths of the sides of the combined rectangular plate are denoted by $2L_x$ and $2L_y$, respectively. We analyze a functionally graded plate as a laminated plate made of n homogeneous layers with different isotropic material properties. Let b_i be the thickness of the ith layer, and coordinate axes x, y, and z are chosen as shown in Fig. 1. Moreover, coordinate z_i represents a local coordinate system

of ith layer, the origin of which is taken at the bottom side of the ith layer. Throughout the paper, the quantities with subscripts $i = 1, 2, \ldots, n$ and $i = n + 1$ denote those for ith layer of laminated plate and piezoelectric plate, respectively. We assume that the combined plate is initially at zero temperature and is suddenly heated from the bottom surface by surrounding media, temperature of which is denoted by the function $T_a f_a(x) g_a(y)$. The relative heat transfer coefficients on bottom and top surfaces of the combined plate are designated h_a and h_b, respectively. We assume that the end surfaces of the combined plate are held at zero temperature. Then, the transient heat conduction equation for the ith layer in dimensionless form is given as

$$\frac{\partial \bar{T}_i}{\partial \tau} = \bar{\kappa}_i \left(\frac{\partial^2 \bar{T}_i}{\partial \bar{x}^2} + \frac{\partial^2 \bar{T}_i}{\partial \bar{y}^2} + \frac{\partial^2 \bar{T}_i}{\partial \bar{z}_i^2} \right); \quad i = 1, \ldots, n \tag{1}$$

$$\frac{\partial \bar{T}_i}{\partial \tau} = \bar{\kappa}_x \frac{\partial^2 \bar{T}_i}{\partial \bar{x}^2} + \bar{\kappa}_y \frac{\partial^2 \bar{T}_i}{\partial \bar{y}^2} + \bar{\kappa}_z \frac{\partial^2 \bar{T}_i}{\partial \bar{z}_i^2}; \quad i = 1 + n \tag{2}$$

and the initial and thermal boundary conditions in dimensionless form are taken in the following forms:

$$\tau = 0; \qquad \bar{T}_i = 0; \quad i = 1, \ldots, (n+1) \tag{3}$$

$$\bar{z}_1 = 0; \qquad \frac{\partial \bar{T}_1}{\partial \bar{z}_1} - H_a \bar{T}_1 = -H_a \bar{T}_a f_a(\bar{x}) g_a(\bar{y}) \tag{4}$$

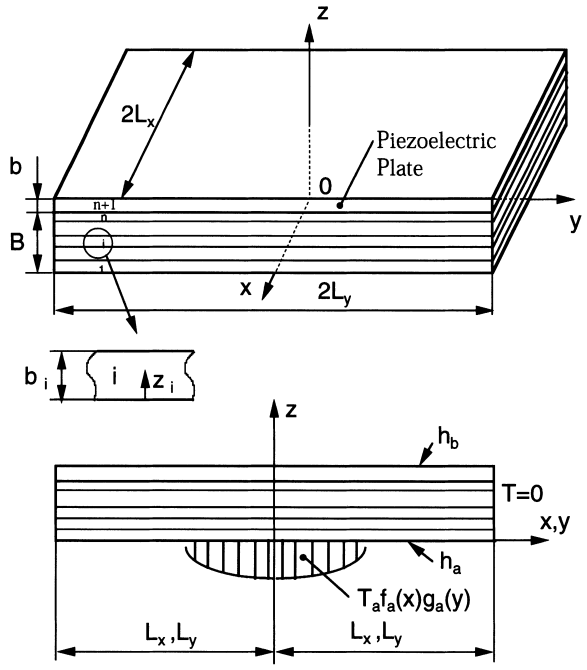

Fig. 1. Analytical model and coordinate system.

$$\bar{z}_i = \bar{b}_i, \quad \bar{z}_{i+1} = 0; \quad \bar{T}_i = \bar{T}_{i+1}; \quad i = 1, \ldots, n \tag{5}$$

$$\bar{z}_i = \bar{b}_i, \quad \bar{z}_{i+1} = 0; \quad \bar{\lambda}_{ti}\frac{\partial \bar{T}_i}{\partial \bar{z}_i} = \bar{\lambda}_{t,\,i+1}\frac{\partial \bar{T}_{i+1}}{\partial \bar{z}_{i+1}}; \quad i = 1, \ldots, (n-1) \tag{6}$$

$$\bar{z}_n = \bar{b}_n, \quad \bar{z}_{n+1} = 0; \quad \bar{\lambda}_{tn}\frac{\partial \bar{T}_n}{\partial \bar{z}_n} = \bar{\lambda}_{tz}\frac{\partial \bar{T}_{n+1}}{\partial \bar{z}_{n+1}}$$

$$\bar{z}_{n+1} = \bar{b}; \qquad \frac{\partial \bar{T}_{n+1}}{\partial \bar{z}_{n+1}} + H_b \bar{T}_{n+1} = 0 \tag{7}$$

$$\bar{x} = \pm \bar{L}_x; \quad \bar{T}_i = 0; \quad i = 1, \ldots, (n+1) \tag{8}$$

$$\bar{y} = \pm \bar{L}_y; \quad \bar{T}_i = 0; \quad i = 1, \ldots, (n+1) \tag{9}$$

In expressions (1)–(9), we have introduced the following dimensionless values:

$$\left(\bar{T}_i, \bar{T}_a, \bar{T}_b\right) = \frac{(T_i, T_a, T_b)}{T_0}, \quad \left(\bar{L}_x, \bar{L}_y, \bar{b}_i, \bar{b}\right) = \frac{\left(L_x, L_y, b_i, b\right)}{B}, \quad (\bar{x}, \bar{y}, \bar{z}, \bar{z}_i) = \frac{(x, y, z, z_i)}{B}$$

$$(\bar{\kappa}_i, \bar{\kappa}_k) = \frac{(\kappa_i, \kappa_k)}{\kappa_0}; \quad k = x, y, z, \quad \left(\bar{\lambda}_{ti}, \bar{\lambda}_z\right) = \frac{(\lambda_{ti}, \lambda_z)}{\lambda_{t0}}, \quad \tau = \frac{\kappa_0 t}{B^2}, \quad (H_a, H_b) = (h_a, h_b)B \tag{10}$$

where T_i is the temperature change of the ith layer; κ_i and $\kappa_k (k = x, y, z)$ are thermal diffusivity; λ_{ti} and λ_{tz} are thermal conductivity; t is time; and T_0, κ_0, and λ_{t0} are typical values of temperature, thermal diffusivity and thermal conductivity, respectively. Moreover, the relation between the local coordinate $\bar{z}_i$ and the global coordinate $\bar{z}$ is given as follows:

$$\bar{z} = \bar{z}_i + \sum_{p=1}^{i-1} \bar{b}_p \tag{11}$$

For the sake of brevity, we introduce the following symmetric conditions for the temperature functions $f_a(\bar{x})$ and $g_a(\bar{y})$ without loss of generality:

$$f_a(-\bar{x}) = f_a(\bar{x}), \qquad g_a(-\bar{y}) = g_a(\bar{y}) \tag{12}$$

To solve the fundamental equations (1) and (2), we introduce the finite cosine transformations with respect to the variables $\bar{x}$ and $\bar{y}$ and Laplace transformation with respect to the variable τ. Performing these integral transformations under the conditions (3), (8) and (9), we obtain

$$\frac{\mathrm{d}^2 \tilde{\bar{T}}_i^*}{\mathrm{d}\bar{z}_i^2} + \left(\frac{\mu^2}{\bar{\kappa}_i} - q^2 - s^2\right)\tilde{\bar{T}}_i^* = 0; \quad i = 1, \ldots, n \tag{13}$$

$$\frac{\mathrm{d}^2\tilde{\hat{\bar{T}}}_i^*}{\mathrm{d}\bar{z}_i^2}+\frac{1}{\bar{\kappa}_z}\left(\omega^2-\bar{\kappa}_x q^2-\bar{\kappa}_y s^2\right)\tilde{\hat{\bar{T}}}_i^*=0;\quad i=1+n \tag{14}$$

where the symbols $(\hat{})$,$(\tilde{})$ and $(^*)$ imply the integral transformations with respect to the variables, $\bar{x}$, $\bar{y}$ and τ, and the parameters of the transformations are denoted by q, s and $P(=-\omega^2)$, respectively. And q and s represent the root of the equations

$$\cos q\bar{L}_x=0,\qquad \cos s\bar{L}_y=0 \tag{15}$$

The solution of Eqs. (13) and (14) is

$$\tilde{\hat{\bar{T}}}_i^*=\begin{cases}A_i\cosh\beta_i\bar{z}_i+B_i\sinh\beta_i\bar{z}_i\\ A_i\cos\gamma_i\bar{z}_i+B_i\sin\gamma_i\bar{z}_i;\quad i=1,\ldots,(n+1)\end{cases} \tag{16}$$

where

$$\beta_i^2=-\left(\frac{\omega^2}{\bar{\kappa}_i}-q^2-s^2\right)\quad \text{if } i=1,\ldots,n \text{ and } \frac{\omega^2}{\bar{\kappa}_i}-q^2-s^2<0$$

$$\gamma_i^2=\frac{\omega^2}{\bar{\kappa}_i}-q_2-s_2\quad \text{if } i=1,\ldots,n \text{ and } \frac{\omega^2}{\bar{\kappa}_i}-q^2-s^2>0$$

$$\beta_i^2=-\frac{\omega^2-\bar{\kappa}_x q^2-\bar{\kappa}_y s^2}{\bar{\kappa}_z}\quad \text{if } i=n+1 \text{ and } \left(\omega^2-\bar{\kappa}_x q^2-\bar{\kappa}_y s^2\right)<0$$

$$\gamma_i^2=\frac{\omega^2-\bar{\kappa}_x q^2-\bar{\kappa}_y s^2}{\bar{\kappa}_z}\quad \text{if } i=n+1 \text{ and } \left(\omega^2-\bar{\kappa}_x q^2-\bar{\kappa}_y s^2\right)>0 \tag{17}$$

and A_i and B_i are unknown constants determined from the boundary conditions. Substituting Eq. (16) into the boundary conditions in the transformed domain from Eqs. (4)–(7), the constants A_i and B_i can be determined making use of Cramer's formula. Then Eq. (16) is

$$\tilde{\hat{\bar{T}}}_i^*=\begin{cases}\dfrac{1}{P\Delta}\left(\bar{A}_i\cosh\beta_i\bar{z}_i+\bar{B}_i\sinh\beta_i\bar{z}_i\right)\\ \dfrac{1}{P\Delta}\left(\bar{A}_i\cos\gamma_i\bar{z}_i+\bar{B}_i\sin\gamma_i\bar{z}_i\right)\end{cases} \tag{18}$$

where Δ is a determinant of $2(n+1)\times 2(n+1)$ matrix $[a_{kl}]$, and the coefficients $\bar{A}_i$ and $\bar{B}_i$ are defined as the determinant of the matrix similar to the coefficient matrix $[a_{kl}]$, in which the $(2i-1)$th column or $2i$th column is exchanged by the constant vector $\{c_k\}$. The nonzero element a_{kl} and c_k among the coefficient matrix $[a_{kl}]$ and the constant vector $\{c_k\}$ are given as follows:

$$a_{11}=-H_a,\qquad a_{12}=\begin{cases}\beta_1\\ \gamma_1\end{cases}$$

$$a_{2i,\,2i-1}=\begin{cases}\cosh\beta_i\bar{b}_i\\ \cos\gamma_i\bar{b}_i\end{cases},\qquad a_{2i,\,2i}=\begin{cases}\sinh\beta_i\bar{b}_i\\ \sin\gamma_i\bar{b}_i\end{cases},\qquad a_{2i,\,2i+1}=-1$$

$$a_{2i+1,\,2i-1}=\begin{cases}\bar{\lambda}_{ti}\beta_i\sinh\beta_i\bar{b}_i\\ -\bar{\lambda}_{ti}\gamma_i\sin\gamma_i b_i\end{cases},\quad a_{2i+1,\,2i}=\begin{cases}\bar{\lambda}_{ti}\beta_i\cosh\beta_j\bar{b}_i\\ \bar{\lambda}_{ti}\gamma_i\cos\gamma_i b_i\end{cases};\quad i=1,\ldots,n$$

$$a_{2i+1,\,2i+2}=\begin{cases}-\bar{\lambda}_{t,\,i+1}\beta_{i+1}\\ -\bar{\lambda}_{t,\,i+1}\gamma_{i+1}\end{cases};\ i=1,\ldots,(n-1),\quad a_{2n+1,\,2n+2}=\begin{cases}-\bar{\lambda}_{tz}\beta_{n+1}\\ -\bar{\lambda}_{tz}\gamma_{n+1}\end{cases}$$

$$a_{2n+2,\,2n+1}=\begin{cases}H_b\cosh\beta_{n+1}\bar{b}+\beta_{n+1}\sinh\beta_{n+1}\bar{b}\\ H_b\cos\gamma_{n+1}\bar{b}-\gamma_{n+1}\sin\gamma_{n+1}\bar{b}\end{cases},\quad a_{2n+2,\,2n+2}=\begin{cases}H_b\sinh\beta_{n+1}\bar{b}+\beta_{n+1}\cosh\beta_{n+1}\bar{b}\\ H_b\sin\gamma_{n+1}\bar{b}+\gamma_{n+1}\cos\gamma_{n+1}\bar{b}\end{cases}$$

$$c_1=-H_a\bar{T}_a\hat{f}_a(q)\tilde{g}_a(s)\tag{19}$$

In Eq. (19), the upper part of elements a_{kl} corresponds to the case of $\omega^2\bar{\kappa}_i-q^2-s^2<0$ or $\omega^2-\bar{\kappa}_x q^2-\bar{\kappa}_y s^2<0$, and the lower part to the case of $\omega^2\bar{\kappa}_i-q^2-s^2>0$ or $\omega^2-\bar{\kappa}_x q^2-\bar{\kappa}_y s^2>0$. Using the residue theorem, we can accomplish the inverse Laplace transformation on Eq. (18). The temperature solution $\bar{\bar{T}}_i$ are given by the summation of the residue. As the single-valued poles of Eq. (18) correspond to $P=0$ and the roots of, $\Delta=0$ the residue for $P=0$ gives a solution for the steady state and the summation of residue for $\Delta=0$ gives a solution for the unsteady state. Accomplishing the inverse finite cosine transformations, the temperature solution $\bar{T}_i$ can be expressed as follows:

$$\bar{T}_i=\sum_{k=1}^{\infty}\sum_{l=1}^{\infty}\bar{T}_{ikl}\cos q_k\bar{x}\cos s_l\bar{y};\quad i=1,\ldots,(n+1)\tag{20}$$

where

$$\bar{T}_{ikl}=\frac{4}{\bar{L}_x\bar{L}_y}\left[\frac{1}{D}\left(\bar{A}_i'\cosh\rho_{kl}\bar{z}_i+\bar{B}_i'\sinh\rho_{kl}\bar{z}_i\right)+\sum_{j=1}^{m}\frac{2\exp\left(-\omega_j^2\tau\right)}{\omega_j\Delta'(\omega_j)}\left(\bar{A}_i\cosh\beta_{ij}\bar{z}_i+\bar{B}_i\sinh\beta_{ij}\bar{z}_i\right)\right.$$
$$\left.+\sum_{j=m+1}^{\infty}\frac{2\exp\left(-\omega_j^2\tau\right)}{\omega_j\Delta'(\omega_j)}\left(\bar{A}_i\cos\gamma_{ij}\bar{z}_i+\bar{B}_i\sin\gamma_{ij}\bar{z}_i\right)\right]\tag{21}$$

and in Eqs. (20) and (21), q_k, s_l, $\Delta'(\omega_j)$, ρ_{kl} are

$$q_k=\frac{(2k-1)\pi}{2\bar{L}_x},\quad s_l=\frac{(2l-1)\pi}{2\bar{L}_y},\quad \Delta'(\omega_j)=\mathrm{d}\Delta/\mathrm{d}\omega|_{\omega=\omega_j}$$

$$\rho_{kl}=\sqrt{q_k^2+s_l^2};\quad i=1,\ldots,n$$

$$\rho_{kl}=\sqrt{\left(\bar{\kappa}_x q_k^2+\bar{\kappa}_y s_l^2\right)/\bar{\kappa}_z};\quad i=n+1\tag{22}$$

and ω_j represent the jth positive roots of the following transcendental equation

$$\Delta(\omega)=0\tag{23}$$

and the condition for the eigenvalue ω_j is given as

$$\omega_1 < \omega_2 < \cdots < \omega_m < \sqrt{\bar{\kappa}_i\left(q_k^2 + s_l^2\right)} < \omega_{m+1} < \cdots \text{ if } i = 1, \ldots, n$$

$$\omega_1 < \omega_2 < \cdots < \omega_m < \sqrt{\bar{\kappa}_x q_k^2 + \bar{\kappa}_y s_l^2} < \omega_{m+1} < \cdots \quad \text{if } i = n+1 \tag{24}$$

Moreover, D is a determinant of $2(n+1) \times 2(n+1)$ matrix $[e_{kl}]$, and the coefficients $\bar{A}_i'$ and $\bar{B}_i'$ are defined as determinants of the matrix similar to the coefficient matrix $[e_{kl}]$, in which the $(2i-1)$th column and $2i$th column are each replaced by the constant vector $\{c_k\}$. The nonzero elements e_{kl} are

$$e_{11} = -H_a, \qquad e_{12} = \rho_{kl}$$

$$e_{2i,\,2i-1} = \cosh \rho_{kl}\bar{b}_i, \quad e_{2i,\,2i} = \sinh \rho_{kl}\bar{b}_i, \quad e_{2i,\,2i+1} = -1$$

$$e_{2i+1,\,2i-1} = \bar{\lambda}_{ti}\rho_{kl}\sinh \rho_{kl}\bar{b}_i, \quad e_{2i+1,\,2i} = \bar{\lambda}_{ti}\rho_{kl}\cosh \rho_{kl}\bar{b}_i; \quad i = 1, \ldots, n$$

$$e_{2i+1,\,2i+2} = -\bar{\lambda}_{t,\,i+1}\rho_{kl}; \quad i = 1, \ldots, (n-1)$$

$$e_{2n+1,\,2n+2} = -\bar{\lambda}_{tz}\rho_{kl}, \quad e_{2n+2,\,2n+1} = H_b\cosh \rho_{kl}\bar{b} + \rho_{kl}\sinh \rho_{kl}\bar{b}$$

$$e_{2n+2,\,2n+2} = H_b\sinh \rho_{kl}\bar{b} + \rho_{kl}\cosh \rho_{kl}\bar{b} \tag{25}$$

4. Piezothermoelasticity problem

We now develop the three-dimensional analysis for transient piezothermoelasticity in the simply supported functionally graded rectangular plate bonded to a piezoelectric plate. We introduce the following dimensionless values.

$$\bar{\sigma}_{kli} = \frac{\sigma_{kli}}{\alpha_0 Y_0 T_0}, \quad \left(\bar{\varepsilon}_{kli}, \bar{\gamma}_{kli}\right) = \frac{(\varepsilon_{kli}, \gamma_{kli})}{\alpha_0 T_0}, \quad (\bar{u}_i, \bar{v}_i, \bar{w}_i) = \frac{(u_i, v_i, w_i)}{\alpha_0 T_0 B}$$

$$\bar{\alpha}_k = \frac{\alpha_k}{\alpha_0}, \quad \bar{C}_{kl} = \frac{C_{kl}}{Y_0}, \quad \bar{E}_k = \frac{E_k|d_1|}{\alpha_0 T_0}, \quad \bar{D}_k = \frac{D_k}{\alpha_0 Y_0 T_0 |d_1|}, \quad \bar{\phi} = \frac{\phi|d_1|}{\alpha_0 T_0 B}$$

$$\bar{e}_{kl} = \frac{e_{kl}}{Y_0|d_1|}, \quad \bar{\eta}_{kl} = \frac{\eta_{kl}}{Y_0|d_1|^2}, \quad \bar{p}_z = \frac{p_z}{\alpha_0 Y_0|d_1|}, \quad \bar{\lambda}_i = \frac{\lambda_i}{Y_0}, \quad \bar{\mu}_i = \frac{\mu_i}{Y_0} \tag{26}$$

where σ_{kli} is the stress component, ε_{kli} is the normal strain component, γ_{kli} is the shearing strain component, (u_i, v_i, w_i) are the displacement components, α_k is the coefficient of linear thermal expansion, C_{kl} is the elastic stiffness constant, E_k is the electric field intensity, D_k is the electric displacement, ϕ is the electric potential, e_{kl} is the piezoelectric coefficient, η_{kl} is the dielectric constant, p_z is the pyroelectric constant, d_1 is the piezoelectric modulus and α_0 and Y_0 are the typical values of the coefficient of linear thermal expansion and Young's modulus of elasticity, respectively. And λ_i and μ_i are Lame's constants.

In the case of FGM plate, the stress–strain relations for the ith layer are expressed in dimensionless form as follows:

$$\begin{Bmatrix} \bar{\sigma}_{xxi} \\ \bar{\sigma}_{yyi} \\ \bar{\sigma}_{zzi} \\ \bar{\sigma}_{yzi} \\ \bar{\sigma}_{zxi} \\ \bar{\sigma}_{xyi} \end{Bmatrix} = \begin{bmatrix} \bar{\lambda}_i + 2\bar{u}_i & \bar{\lambda}_i & \bar{\lambda}_i & 0 & 0 & 0 \\ \bar{\lambda}_i & \bar{\lambda}_i + 2\bar{\mu}_i & \bar{\lambda}_i & 0 & 0 & 0 \\ \bar{\lambda}_i & \bar{\lambda}_i & \bar{\lambda}_i + 2\bar{\mu}_i & 0 & 0 & 0 \\ 0 & 0 & 0 & \bar{\mu}_i & 0 & 0 \\ 0 & 0 & 0 & 0 & \bar{\mu}_i & 0 \\ 0 & 0 & 0 & 0 & 0 & \bar{\mu}_i \end{bmatrix} \begin{Bmatrix} \bar{\varepsilon}_{xxi} - \bar{\alpha}_i \bar{T}_i \\ \bar{\varepsilon}_{yyi} - \bar{\alpha}_i \bar{T}_i \\ \bar{\varepsilon}_{zzi} - \bar{\alpha}_i \bar{T}_i \\ \bar{\gamma}_{yzi} \\ \bar{\gamma}_{zxi} \\ \bar{\gamma}_{xyi} \end{Bmatrix}; \quad i = 1, \ldots, n \tag{27}$$

In the case of the piezoelectric plate, the stress–strain relations are expressed in dimensionless form as follows:

$$\begin{Bmatrix} \bar{\sigma}_{xxi} \\ \bar{\sigma}_{yyi} \\ \bar{\sigma}_{zzi} \\ \bar{\sigma}_{yzi} \\ \bar{\sigma}_{zxi} \\ \bar{\sigma}_{xyi} \end{Bmatrix} = \begin{bmatrix} \bar{C}_{11} & \bar{C}_{12} & \bar{C}_{13} & 0 & 0 & 0 \\ \bar{C}_{12} & \bar{C}_{22} & \bar{C}_{23} & 0 & 0 & 0 \\ \bar{C}_{13} & \bar{C}_{23} & \bar{C}_{33} & 0 & 0 & 0 \\ 0 & 0 & 0 & \bar{C}_{44} & 0 & 0 \\ 0 & 0 & 0 & 0 & \bar{C}_{55} & 0 \\ 0 & 0 & 0 & 0 & 0 & \bar{C}_{66} \end{bmatrix} \begin{Bmatrix} \bar{\varepsilon}_{xxi} - \bar{\alpha}_x \bar{T}_i \\ \bar{\varepsilon}_{yyi} - \bar{\alpha}_y \bar{T}_i \\ \bar{\varepsilon}_{zzi} - \bar{\alpha}_z \bar{T}_i \\ \bar{\gamma}_{yzi} \\ \bar{\gamma}_{zxi} \\ \bar{\gamma}_{xyi} \end{Bmatrix} - \begin{bmatrix} 0 & 0 & \bar{e}_{31} \\ 0 & 0 & \bar{e}_{32} \\ 0 & 0 & \bar{e}_{33} \\ 0 & \bar{e}_{24} & 0 \\ \bar{e}_{15} & 0 & 0 \\ 0 & 0 & 0 \end{bmatrix} \begin{Bmatrix} \bar{E}_x \\ \bar{E}_y \\ \bar{E}_z \end{Bmatrix}; \tag{28}$$

$$i = n + 1$$

The constitutive equations for the electric field are

$$\bar{D}_x = \bar{e}_{15}\bar{\gamma}_{zx} + \bar{\eta}_{11}\bar{E}_x, \quad \bar{D}_y = \bar{e}_{24}\bar{\gamma}_{yz} + \bar{\eta}_{22}\bar{E}_y, \quad \bar{D}_z = \bar{e}_{31}\bar{\varepsilon}_{xx} + \bar{e}_{32}\bar{\varepsilon}_{yy} + \bar{e}_{33}\bar{\varepsilon}_{zz} + \bar{\eta}_{33}\bar{E}_z + \bar{p}_z\bar{T}_{n+1} \tag{29}$$

The relations between the electric field intensities and the electric potential ϕ are defined by

$$\bar{E}_x = -\bar{\phi}_{,\,\bar{x}}, \quad \bar{E}_y = -\bar{\phi}_{,\,\bar{y}}, \quad \bar{E}_z = -\bar{\phi}_{,\,\bar{z}} \tag{30}$$

where a comma denotes partial differentiation with respect to the variable it follows. If the free charge is absent, the equation of electrostatics is expressed in dimensionless form as follows:

$$\bar{D}_{x,\,\bar{x}} + \bar{D}_{y,\,\bar{y}} + \bar{D}_{z,\,\bar{z}} = 0 \tag{31}$$

The displacement–strain relations for the ith layer are expressed in dimensionless form as follows:

$$\bar{\varepsilon}_{xxi} = \bar{u}_{i,\,\bar{x}}, \quad \bar{\varepsilon}_{yyi} = \bar{v}_{i,\,\bar{y}}, \quad \bar{\varepsilon}_{zzi} = \bar{w}_{i,\,\bar{z}}$$

$$\bar{\gamma}_{xyi} = \bar{u}_{i,\,\bar{y}} + \bar{v}_{i,\,\bar{x}}, \quad \bar{\gamma}_{yzi} = \bar{v}_{i,\,\bar{z}} + \bar{w}_{i,\,\bar{y}}, \quad \bar{\gamma}_{zxi} = \bar{u}_{i,\,\bar{z}} + \bar{w}_{i,\,\bar{x}}; \quad i = 1, \ldots, (n+1) \tag{32}$$

The equilibrium equations for the ith layer are expressed in dimensionless form as follows:

$$\bar{\sigma}_{xxi,\,\bar{x}} + \bar{\sigma}_{xyi,\,\bar{y}} + \bar{\sigma}_{zxi,\,\bar{z}} = 0, \quad \bar{\sigma}_{xyi,\,\bar{x}} + \bar{\sigma}_{yyi,\,\bar{y}} + \bar{\sigma}_{yzi,\,\bar{z}} = 0$$

$$\bar{\sigma}_{zxi,\,\bar{x}} + \bar{\sigma}_{yzi,\,\bar{y}} + \bar{\sigma}_{zzi,\,\bar{z}} = 0; \quad i = 1, \ldots, (n+1) \tag{33}$$

In the case of FGM plate, substituting Eq. (32) into Eq. (27), and later into Eq. (33), the displacement equations of equilibrium are written as

$$(\bar{\lambda}_i+2\bar{\mu}_i)\bar{u}_{i,\overline{xx}}+\bar{\mu}_i(\bar{u}_{i,\overline{yy}}+\bar{u}_{i,\overline{zz}})+(\bar{\lambda}_i+\bar{\mu}_i)(\bar{v}_{i,\overline{xy}}+\bar{w}_{i,\overline{xz}})=(3\bar{\lambda}_i+2\bar{\mu}_i)\bar{\alpha}_i\bar{T}_{i,\bar{x}}$$

$$(\bar{\lambda}_i+\bar{\mu}_i)(\bar{u}_{i,\overline{xy}}+\bar{w}_{i,\overline{yz}})+\bar{\mu}_i(\bar{v}_{i,\overline{xx}}+\bar{v}_{i,\overline{zz}})+(\bar{\lambda}_i+2\bar{\mu}_i)\bar{v}_{i,\overline{yy}}=(3\bar{\lambda}_i+2\bar{\mu}_i)\bar{\alpha}_i\bar{T}_{i,\bar{y}}$$

$$(\bar{\lambda}_i+\bar{\mu}_i)(\bar{u}_{i,\overline{xz}}+\bar{v}_{i,\overline{yz}})+\bar{\mu}_i(\bar{w}_{i,\overline{xx}}+\bar{w}_{i,\overline{yy}})+(\bar{\lambda}_i+2\bar{\mu}_i)\bar{w}_{i,\overline{zz}}=(3\bar{\lambda}_i+2\bar{\mu}_i)\bar{\alpha}_i\bar{T}_{i,\bar{z}};\quad i=1,\ldots,n \tag{34}$$

In the case of the piezoelectric plate, substituting Eqs. (30) and (32) into Eq. (28), and later into Eqs. (31) and (33), the governing equations of the displacement components and the electric potential ϕ in dimensionless form are written as

$$\begin{aligned}
&\bar{C}_{11}\bar{u}_{n+1,\overline{xx}}+\bar{C}_{66}\bar{u}_{n+1,\overline{yy}}+\bar{C}_{55}\bar{u}_{n+1,\overline{zz}}+(\bar{C}_{12}+\bar{C}_{66})\bar{v}_{n+1,\overline{xy}}+(\bar{C}_{13}+\bar{C}_{55})\bar{w}_{n+1,\overline{xz}}+(\bar{e}_{31}\\
&\quad+\bar{e}_{15})\bar{\phi}_{,\overline{xz}}=\left(\bar{C}_{11}\bar{\alpha}_x+\bar{C}_{12}\bar{\alpha}_y+\bar{C}_{13}\bar{\alpha}_z\right)\bar{T}_{n+1,\bar{x}}\\
&(\bar{C}_{66}+\bar{C}_{12})\bar{u}_{n+1,\overline{xy}}+\bar{C}_{66}\bar{v}_{n+1,\overline{xx}}+\bar{C}_{22}\bar{v}_{n+1,\overline{yy}}+\bar{C}_{44}\bar{v}_{n+1,\overline{zz}}\\
&\quad+(\bar{C}_{23}+\bar{C}_{44})\bar{w}_{n+1,\overline{yz}}+(e_{32}+\bar{e}_{24})\bar{\phi}_{,\overline{yz}}=\left(\bar{C}_{12}\bar{\alpha}_x+\bar{C}_{22}\bar{\alpha}_y+\bar{C}_{23}\bar{\alpha}_z\right)\bar{T}_{n+1,\bar{y}}\\
&(\bar{C}_{13}+\bar{C}_{55})\bar{u}_{n+1,\overline{xz}}+(\bar{C}_{44}+\bar{C}_{23})\bar{v}_{n+1,\overline{yz}}+\bar{C}_{55}\bar{w}_{n+1,\overline{xx}}\\
&\quad+\bar{C}_{44}\bar{w}_{n+1,\overline{yy}}+(\bar{C}_{33}+\bar{w}_{n+1,\overline{zz}}+(\bar{e}_{15})\bar{\phi}_{,\overline{xx}}+\bar{e}_{24}\bar{\phi}_{,\overline{yy}}+\bar{e}_{33}\bar{\phi}_{,\overline{zz}}=\left(\bar{C}_{13}\bar{\alpha}_x+\bar{C}_{23}\bar{\alpha}_y+\bar{C}_{33}\bar{\alpha}_z\right)\bar{T}_{n+1,\bar{z}}\\
&(\bar{e}_{15}+\bar{e}_{31})\bar{u}_{n+1,\overline{xz}}+(\bar{e}_{24}+\bar{e}_{32})\bar{v}_{n+1,\overline{yz}}+\bar{e}_{15}\bar{w}_{n+1,\overline{xx}}\\
&\quad+\bar{e}_{24}\bar{w}_{n+1,\overline{yy}}+\bar{e}_{33}\bar{w}_{n+1,\overline{zz}}-\bar{\eta}_{11}\bar{\phi}_{,\overline{xx}}-\bar{\eta}_{22}\bar{\phi}_{,\overline{yy}}-\bar{\eta}_{33}\bar{\phi}_{,\overline{zz}}=-\bar{p}_z\bar{T}_{n+1,\bar{z}}
\end{aligned} \tag{35}$$

If the bottom and top surfaces of the combined plate are traction free, and the interfaces of each layer are perfectly bonded, then the boundary conditions of bottom and top surfaces and the conditions of continuity at the interfaces can be represented as follows:

$$\bar{z}_1=0;\quad \bar{\sigma}_{zz1}=0,\quad \bar{\sigma}_{zx1}=0,\quad \bar{\sigma}_{yz1}=0$$

$$\bar{z}_i=\bar{b}_i,\quad \bar{z}_{i+1}=0;\quad \bar{\sigma}_{zzi}=\bar{\sigma}_{zz,\,i+1},\quad \bar{\sigma}_{zxi}=\bar{\sigma}_{zx,\,i+1},\quad \bar{\sigma}_{yzi}=\bar{\sigma}_{yz,\,i+1}$$

$$\bar{u}_i=\bar{u}_{i+1},\quad \bar{v}_i=\bar{v}_{i+1},\ \bar{w}_i=\bar{w}_{i+1};\quad i=1,\ldots,n$$

$$\bar{z}_{n+1}=\bar{b};\quad \bar{\sigma}_{zz,\,n+1}=0,\quad \bar{\sigma}_{zx,\,n+1}=0,\quad \bar{\sigma}_{yz,\,n+1}=0 \tag{36}$$

The boundary conditions in the thickness direction for the electric field are expresses by

$$\bar{z}_{n+1}=0;\qquad \bar{\phi}=0$$

$$\bar{z}_{n+1}=\bar{b};\qquad \bar{D}_z=0 \tag{37}$$

We now consider the case of a simply supported plate and assume that the end surfaces of piezoelectric rectangular plate are electrically grounded. The boundary conditions are given as follows:

$$\bar{x} = \pm \bar{L}_x; \quad \bar{\sigma}_{xxi} = 0, \quad \bar{v}_i = 0, \quad \bar{w}_i = 0, \quad \bar{\phi} = 0$$

$$\bar{y} = \pm \bar{L}_y; \quad \bar{\sigma}_{yyi} = 0, \quad \bar{u}_i = 0, \quad \bar{w}_i = 0, \quad \bar{\phi} = 0 \tag{38}$$

The boundary conditions (38) are satisfied automatically if the displacement components and electric potential are given the following forms:

$$\bar{u}_i = \sum_{k=1}^{\infty}\sum_{l=1}^{\infty}\left[U_{cikl}(\bar{z}_i) + U_{pikl}(\bar{z}_i)\right]\sin q_k\bar{x}\cos s_l\bar{y}$$

$$\bar{v}_i = \sum_{k=1}^{\infty}\sum_{l=1}^{\infty}\left[V_{cikl}(\bar{z}_i) + V_{pikl}(\bar{z}_i)\right]\cos q_k\bar{x}\sin s_l\bar{y}$$

$$\bar{w}_i = \sum_{k=1}^{\infty}\sum_{l=1}^{\infty}\left[W_{cikl}(\bar{z}_i) + W_{pikl}(\bar{z}_i)\right]\cos q_k\bar{x}\cos s_l\bar{y}; \quad i = 1,\ldots,(n+1)$$

$$\bar{\phi} = \sum_{k=1}^{\infty}\sum_{l=1}^{\infty}\left[\Phi_{ckl}(\bar{z}_{n+1}) + \Phi_{pkl}(\bar{z}_{n+1})\right]\cos q_k\bar{x}\cos s_l\bar{y} \tag{39}$$

In expressions (39), the first term of right-hand side shows the homogeneous solution of Eq. (34) or Eq. (35) and the second term of right-hand side shows the particular solution of Eq. (34) or (35).

In the case of FGM plate, $U_{cikl}(\bar{z}_i)$, $V_{cikl}(\bar{z}_i)$ and $W_{cikl}(\bar{z}_i)$ are given by the following expressions (Pagano, 1970):

$$U_{cikl}(\bar{z}_i) = \left(a_{11}^{(i)} + a_{31}^{(i)}\bar{z}_i + a_{51}^{(i)}\bar{z}_i^2\right)\exp(\rho_{kl}\bar{z}_i) + \left(a_{21}^{(i)} + a_{41}^{(i)}\bar{z}_i + a_{61}^{(i)}\bar{z}_i^2\right)\exp(-\rho_{kl}\bar{z}_i)$$

$$V_{cikl}(\bar{z}_i) = \left(a_{12}^{(i)} + a_{32}^{(i)}\bar{z}_i + a_{52}^{(i)}\bar{z}_i^2\right)\exp(\rho_{kl}\bar{z}_i) + \left(a_{22}^{(i)} + a_{42}^{(i)}\bar{z}_i + a_{62}^{(i)}\bar{z}_i^2\right)\exp(-\rho_{kl}\bar{z}_i)$$

$$W_{cikl}(\bar{z}_i) = \left(a_{13}^{(i)} + a_{33}^{(i)}\bar{z}_i + a_{53}^{(i)}\bar{z}_i^2\right)\exp(\rho_{kl}\bar{z}_i) + \left(a_{23}^{(i)} + a_{43}^{(i)}\bar{z}_i + a_{63}^{(i)}\bar{z}_i^2\right)\exp(-\rho_{kl}\bar{z}_i); \quad i = l,\ldots,n \tag{40}$$

In the above expressions (40), $a_{kl}^{(i)}$ are unknown constants and the following relations among these constants exist

$$a_{5l}^{(i)} = a_{6l}^{(i)} = 0; \quad l = 1, 2, 3$$

$$a_{32}^{(i)} = \frac{s_l}{q_k}a_{31}^{(i)}, \quad a_{33}^{(i)} = -\frac{\rho_{kl}}{q_k}a_{31}^{(i)}, \quad a_{42}^{(i)} = \frac{s_l}{q_k}a_{41}^{(i)}, \quad a_{43}^{(i)} = \frac{\rho_{kl}}{q_k}a_{41}^{(i)}$$

$$a_{31}^{(i)} = \frac{q_k\left(\bar{\lambda}_i + \bar{\mu}_i\right)}{\rho_{kl}\left(\bar{\lambda}_i + 3\bar{\mu}_i\right)}\left(q_k a_{11}^{(i)} + s_l a_{12}^{(i)} + \rho_{kl} a_{13}^{(i)}\right)$$

$$a_{41}^{(i)} = -\frac{q_k\left(\bar{\lambda}_i + \bar{\mu}_i\right)}{\rho_{kl}\left(\bar{\lambda}_i + 3\bar{\mu}_i\right)}\left(q_k a_{21}^{(i)} + s_l a_{22}^{(i)} - \rho_{kl} a_{23}^{(i)}\right); \quad i = l, \ldots, n \tag{41}$$

In the case of the piezoelectric plate, $U_{cikl}(\bar{z}_i)$, $V_{cikl}(\bar{z}_i)$, $W_{cikl}(\bar{z}_i)$ and $\bar{\Phi}_{ckl}(\bar{z}_i)$ are given based on Heyliger's solution (Heyliger, 1997). Assuming that

$$\left\{U_{cikl}(\bar{z}_i), V_{cikl}(\bar{z}_i), W_{cikl}(\bar{z}_i), \Phi_{ckl}(\bar{z}_i)\right\} = \left(U^0_{ckl}, V^0_{ckl}, W^0_{ckl}, \Phi^0_{ckl}\right)\exp(p\bar{z}_i); \quad i = n+1 \tag{42}$$

and substituting the homogeneous solution into the homogeneous form of Eq. (35) leads to the next equations.

$$\begin{bmatrix} A_{11} - \bar{C}_{55}p^2 & A_{12} & A_{13}p & A_{14}p \\ A_{12} & A_{22} - \bar{C}_{44}p^2 & A_{23}p & A_{24}p \\ -A_{13}p & -A_{23}p & A_{33} - \bar{C}_{33}p^2 & A_{34} - \bar{e}_{33}p^2 \\ -A_{14}p & -A_{24}p & A_{34} - \bar{e}_{33}p^2 & A_{44} + \bar{\eta}_{33}p^2 \end{bmatrix} \begin{Bmatrix} U^0_{ckl} \\ V^0_{ckl} \\ W^0_{ckl} \\ \Phi^0_{ckl} \end{Bmatrix} = \begin{Bmatrix} 0 \\ 0 \\ 0 \\ 0 \end{Bmatrix} \tag{43}$$

where

$$A_{11} = \bar{C}_{11}q_k^2 + \bar{C}_{66}s_l^2, \quad A_{12} = \left(\bar{C}_{12} + \bar{C}_{66}\right)q_k s_l, \quad A_{13} = \left(\bar{C}_{13} + \bar{C}_{55}\right)q_k, \quad A_{14} = (\bar{e}_{31} + \bar{e}_{15})q_k$$

$$A_{22} = \bar{C}_{66}q_k^2 + \bar{C}_{22}s_l^2, \quad A_{23} = \left(\bar{C}_{23} + \bar{C}_{44}\right)s_l, \quad A_{24} = (\bar{e}_{32} + \bar{e}_{24})s_l, \quad A_{33} = \bar{C}_{55}q_k^2 + \bar{C}_{44}s_l^2$$

$$A_{34} = \bar{e}_{15}q_k^2 + \bar{e}_{24}s_l^2, \quad A_{44} = -\left(\bar{\eta}_{11}q_k^2 + \bar{\eta}_{22}s_l^2\right) \tag{44}$$

Non-trivial solutions of Eq. (43) exist if the determinant of the coefficient vanishes, which leads to the eighth-order equation of p. This equation can be written as the fourth-order equation

$$r^4 + cr^3 + dr^2 + er + f = 0 \tag{45}$$

where

$$r = p^2$$

$$c = \frac{1}{A}\left\{\bar{\eta}_{33}\left[\bar{C}_{44}\left(A_{11}\bar{C}_{33} - A_{13}^2\right) + \bar{C}_{55}\left(A_{33}\bar{C}_{44} + A_{22}\bar{C}_{33} - A_{23}^2\right)\right] + \bar{e}_{33}^2\left(A_{11}\bar{C}_{44} + A_{22}\bar{C}_{55}\right)\right.$$
$$\left. + 2\bar{e}_{33}\left[\bar{C}_{55}\left(A_{34}\bar{C}_{44} - A_{23}A_{24}\right) - A_{13}A_{14}\bar{C}_{44}\right] + \bar{C}_{33}\left[\bar{C}_{55}\left(A_{24}^2 - A_{44}\bar{C}_{44}\right) + A_{14}^2\bar{C}_{44}\right]\right\}$$

$$d=\frac{1}{A}\Big\{\bar{\eta}_{33}\Big[A_{11}A_{23}^2+A_{13}^2A_{22}-2A_{12}A_{23}A_{13}-A_{33}\big(A_{11}\bar{C}_{44}+A_{22}\bar{C}_{55}\big)+\bar{C}_{33}\big(A_{12}^2-A_{11}A_{22}\big)\Big]$$
$$+2\bar{e}_{33}\big(A_{13}A_{22}A_{14}+A_{11}A_{23}A_{24}-A_{12}A_{23}A_{14}-A_{12}A_{24}A_{13}-A_{11}A_{34}\bar{C}_{44}-A_{22}A_{34}\bar{C}_{55}\big)+\bar{e}_{33}^2\big(A_{12}^2$$
$$-A_{11}A_{22}\big)+\bar{C}_{55}\Big(2A_{23}A_{24}A_{34}+A_{22}A_{44}\bar{C}_{33}+A_{33}A_{44}\bar{C}_{44}-A_{23}^2A_{44}-A_{24}^2A_{33}-A_{34}^2\bar{C}_{44}\Big)$$
$$+\bar{C}_{44}\Big(A_{11}A_{44}\bar{C}_{33}-A_{13}^2A_{44}+2A_{13}A_{14}A_{34}-A_{14}^2A_{33}\Big)+(A_{13}A_{24}-A_{14}A_{23})^2\Big\}$$

$$e=\frac{1}{A}\Big\{\big(A_{11}A_{22}-A_{12}^2\big)\big(\bar{\eta}_{33}A_{33}+2\bar{e}_{33}A_{34}-\bar{C}_{33}A_{44}\big)+\big(A_{34}^2-A_{33}A_{44}\big)\big(\bar{C}_{55}A_{22}+\bar{C}_{44}A_{11}\big)$$
$$+2\big[A_{12}A_{24}(A_{13}A_{34}-A_{14}A_{33})+A_{12}A_{23}(A_{14}A_{34}-A_{13}A_{44})-A_{34}(A_{11}A_{23}A_{24}+A_{13}A_{22}A_{14})\big]$$
$$+A_{33}\big(A_{11}A_{24}^2+A_{14}^2A_{22}\big)+A_{44}\big(A_{13}^2A_{22}+A_{11}A_{23}^2\big)\Big\}$$

$$f=\frac{1}{A}\big(A_{34}A_{44}-A_{34}^2\big)\big(A_{11}A_{22}-A_{12}^2\big)$$

$$A=-\bar{C}_{55}\bar{C}_{44}\Big(\bar{C}_{33}\bar{\eta}_{33}+\bar{e}_{33}^2\Big) \tag{46}$$

From Eq. (45), there might be four real roots, two real roots and one pair of conjugate complex roots, or two pairs of conjugate complex roots.

Case 1 (Real roots for r)**.** Given N real roots for r, $U_{cikl}(\bar{z}_i)$,$V_{cikl}(\bar{z}_i)$, $W_{cikl}(\bar{z}_i)$ and $\Phi_{ckl}(\bar{z}_i)$ are given by the following expressions:

$$U_{cikl}(\bar{z}_i)=\sum_{J=1}^{N}U_{klJ}(\bar{z}_i),\qquad V_{cikl}(\bar{z}_i)=\sum_{J=1}^{N}L_{klJ}U_{klJ}(\bar{z}_i)$$

$$W_{cikl}(\bar{z}_i)=\sum_{J=1}^{N}M_{klJ}W_{klJ}(\bar{z}_i),\qquad \Phi_{ckl}(\bar{z}_i)=\sum_{J=1}^{N}N_{klJ}W_{klJ}(\bar{z}_i);\quad i=n+1 \tag{47}$$

where

$$U_{klJ}(\bar{z}_i)=F_{klJ}C_{klJ}(\bar{z}_i)+G_{klJ}S_{klJ}(\bar{z}_i)$$

$$W_{klJ}(\bar{z}_i)=G_{klJ}C_{klJ}(\bar{z}_i)+\alpha_{klJ}F_{klJ}S_{klJ}(\bar{z}_i) \tag{48}$$

$$L_{klJ}=\frac{1}{D_J}\big(f_{11}m_J^4+\alpha_{klJ}f_{12}m_J^2+f_{13}\big),\qquad M_{klJ}=\frac{m_J}{D_J}\big(f_{21}m_J^4+\alpha_{klJ}f_{22}m_J^2+f_{23}\big)$$

$$N_{klJ}=\frac{m_J}{D_J}\big(f_{31}m_J^4+\alpha_{klJ}f_{32}m_J^2+f_{33}\big),\qquad D_J=\alpha_{klJ}g_1m_J^6+g_2m_J^4+\alpha_{klJ}g_3m_J^2+g_4 \tag{49}$$

$$C_{klJ}(\bar{z}_i)=\cosh(m_J\bar{z}_i),\quad S_{klJ}(\bar{z}_i)=\sinh(m_J\bar{z}_i),\quad m_J=\sqrt{r_J},\quad \alpha_{klJ}=1\quad \text{if } r_J>0$$

$$C_{klJ}(\bar{z}_i)=\cos(m_J\bar{z}_i),\quad S_{klJ}(\bar{z}_i)=\sin(m_J\bar{z}_i),\quad m_J=\sqrt{-r_J},\quad \alpha_{klJ}=-1\quad \text{if } r_J<0 \tag{50}$$

Here F_{klJ} and G_{klJ} are unknown constants. Expressions for the coefficients in Eq. (49) are given in Appendix A.

Case 2 (Complex roots for r)**.** If the complex root for r is expressed by $r_J=\alpha_J\pm j\beta_J$ where $j=\sqrt{-1}$, then the final roots for p are

$$p_J=\pm(a_J+jb_J) \tag{51}$$

where

$$a_J=\left(\alpha_J^2+\beta_J^2\right)^{1/4}\cos\left[\frac{1}{2}\left(\tan^{-1}\frac{\beta_J}{\alpha_J}\right)\right],\qquad b_J=\left(\alpha_J^2+\beta_J^2\right)^{1/4}\sin\left[\frac{1}{2}\left(\tan^{-1}\frac{\beta_J}{\alpha_J}\right)\right] \tag{52}$$

Given J' pairs of complex roots for r, $U_{cikl}(\bar{z}_i)$, $V_{cikl}(\bar{z}_i)$, $W_{cikl}(\bar{z}_i)$ and $\Phi_{ckl}(\bar{z}_i)$ are given by the following expressions:

$$U_{cikl}(\bar{z}_i)=\sum_{J=1}^{J'}U_{klJ}(\bar{z}_i),\qquad V_{cikl}(\bar{z}_i)=\sum_{J=1}^{J'}V_{klJ}(\bar{z}_i)$$

$$W_{cikl}(\bar{z}_i)=\sum_{J=1}^{J'}W_{klJ}(\bar{z}_i),\qquad \Phi_{ckl}(\bar{z}_i)=\sum_{J=1}^{J'}\Phi_{klJ}(\bar{z}_i);\quad i=n+1 \tag{53}$$

where

$$U_{klJ}(\bar{z}_i)=C_{1J}\exp\left(a_J\bar{z}_j\right)\cos b_J\bar{z}_i+C_{2J}\exp(a_J\bar{z}_i)\sin b_J\bar{z}_i+C_{3J}\exp(-a_J\bar{z}_i)\cos b_J\bar{z}_i+C_{4J}\exp(-a_J\bar{z}_i)\times\sin b_J\bar{z}_i$$

$$V_{klJ}(\bar{z}_i)=C_{1J}\exp(a_J\bar{z}_i)(\Gamma_{1J}\cos b_J\bar{z}_i-\Omega_{1J}\sin b_J\bar{z}_i)+C_{2J}\exp(a_J\bar{z}_i)(\Omega_{1J}\cos b_J\bar{z}_i+\Gamma_{1J}\sin b_J\bar{z}_i)+C_{3J}\exp(-a_J\bar{z}_i)(\Gamma_{1J}\cos b_J\bar{z}_i+\Omega_{1J}\sin b_J\bar{z}_i)+C_{4J}\exp(-a_J\bar{z}_i)(-\Omega_{1J}\cos b_J\bar{z}_i+\Gamma_{1J}\sin b_J\bar{z}_i)$$

$$W_{klJ}(\bar{z}_i)=C_{1J}\exp(a_J\bar{z}_i)\left[(a_J\Gamma_{2J}-b_J\Omega_{2J})\cos b_J\bar{z}_i-(b_J\Gamma_{2J}+a_J\Omega_{2J})\sin b_J\bar{z}_i\right]+C_{2J}\exp(a_J\bar{z}_i)\left[(b_J\Gamma_{2J}+a_J\Omega_{2J})\cos b_J\bar{z}_i+(a_J\Gamma_{2J}-b_J\Omega_{2J})\sin b_J\bar{z}_i\right]+C_{3J}\exp(-a_J\bar{z}_i)\left[(b_J\Omega_{2J}-a_J\Gamma_{2J})\cos b_J\bar{z}_i-(b_J\Gamma_{2J}+a_J\Omega_{2J})\sin b_J\bar{z}_i\right]+C_{4J}\exp(-a_J\bar{z}_i)\left[(b_J\Gamma_{2J}+a_J\Omega_{2J})\cos b_J\bar{z}_i+(-a_J\Gamma_{2J}+a_J\Omega_{2J})\times\sin b_J\bar{z}_i\right]$$

$$\Phi_{klJ}(\bar{z}_i) = C_{1J}\exp(a_J\bar{z}_i)\big[(a_J\Gamma_{3J} - b_J\Omega_{3J})\cos b_J\bar{z}_i - (b_J\Gamma_{3J} + a_J\Omega_{3J})\sin b_J\bar{z}_i\big] + C_{2J}\exp(a_J\bar{z}_i)\big[(b_J\Gamma_{3J} + a_J\Omega_{3J})\cos b_J\bar{z}_i + (a_J\Gamma_{3J} - b_J\Omega_{3J})\sin b_J\bar{z}_i\big] + C_{3J}\exp(-a_J\bar{z}_i)\big[(b_J\Omega_{3J} - a_J\Gamma_{3J})\cos b_J\bar{z}_i - (b_J\Gamma_{3J} + a_J\Omega_{3J})\sin b_J\bar{z}_i\big] + C_{4J}\exp(-a_J\bar{z}_i)\big[(b_J\Gamma_{3J} + a_J\Omega_{3J})\cos b_J\bar{z}_i + (-a_J\Gamma_{3J} + b_J\Omega_{3J})\sin b_J\bar{z}_i\big] \tag{54}$$

$$\Gamma_{IJ} = R_e\left[\frac{1}{D(p_J)}\big(f_{I1}p_J^4 + f_{I2}p_J^2 + f_{I3}\big)|_{p_J=a_J+jb_J}\right]$$

$$\Omega_{IJ} = I_m\left[\frac{1}{D(p_J)}\big(f_{I1}p_J^4 + f_{I2}p_J^2 + f_{I3}\big)|_{p_J=a_J+jb_J}\right]; \; I = 1, 2, 3$$

$$D(p_J) = g_1p_J^6 + g_2p_J^4 + g_3p_J^2 + g_4 \tag{55}$$

Here C_{1J}–C_{4J} are unknown constants.

On the other hand, $U_{pikl}(\bar{z}_i)$, $V_{pikl}(\bar{z}_i)$, $W_{pikl}(\bar{z}_i)$ and $\Phi_{pkl}(\bar{z}_i)$ of the particular solutions are obtained as follows:

$$U_{pikl}(\bar{z}_i) = A_{1ikl}\cosh\rho_{kl}\bar{z}_i + A_{2ikl}\sinh\rho_{kl}\bar{z}_i + \sum_{j=1}^{m}\Big(A_{3ikl}^{(j)}\cosh\beta_{ij}\bar{z}_i + A_{4ikl}^{(j)}\sinh\beta_{ij}\bar{z}_i\Big) + \sum_{j=m+1}^{\infty}\Big(A_{5ikl}^{(j)}\cos\gamma_{ij}\bar{z}_i + A_{6ikl}^{(j)}\sin\gamma_{ij}\bar{z}_i\Big)$$

$$V_{pikl}(\bar{z}_i) = B_{1ikl}\cosh\rho_{kl}\bar{z}_i + B_{2ikl}\sinh\rho_{kl}\bar{z}_i + \sum_{j=1}^{m}\Big(B_{3ikl}^{(j)}\cosh\beta_{ij}\bar{z}_i + B_{4ikl}^{(j)}\sinh\beta_{ij}\bar{z}_i\Big) + \sum_{j=m+1}^{\infty}\Big(B_{5ikl}^{(j)}\cos\gamma_{ij}\bar{z}_i + B_{6ikl}^{(j)}\sin\gamma_{ij}\bar{z}_i\Big)$$

$$W_{pikl}(\bar{z}_i) = C_{1ikl}\cosh\rho_{kl}\bar{z}_i + C_{2ikl}\sinh\rho_{kl}\bar{z}_i + \sum_{j=1}^{m}\Big(C_{3ikl}^{(j)}\cosh\beta_{ij}\bar{z}_i + C_{4ikl}^{(j)}\sinh\beta_{ij}\bar{z}_i\Big) + \sum_{j=m+1}^{\infty}\Big(C_{5ikl}^{(j)} \times \cos\gamma_{ij}\bar{z}_i + C_{6ikl}^{(j)}\sin\gamma_{ij}\bar{z}_i\Big); \quad i = 1, \ldots, (n+1)$$

$$\Phi_{pkl}(\bar{z}_{n+1}) = D_{1kl}\cosh\rho_{kl}\bar{z}_{n+1} + D_{2kl}\sinh\rho_{kl}\bar{z}_{n+1} + \sum_{j=1}^{m}\Big[D_{3kl}^{(j)}\cosh\beta_{n+1,\,j}\bar{z}_{n+1} + D_{4kl}^{(j)} \times \sinh\beta_{n+1,\,j}\bar{z}_{n+1}\Big] + \sum_{j=m+1}^{\infty}\Big[D_{5kl}^{(j)}\cos\gamma_{n+1,\,j}\bar{z}_{n+1} + D_{6kl}^{(j)}\sin\gamma_{n+i,\,j}\bar{z}_{n+1}\Big] \tag{56}$$

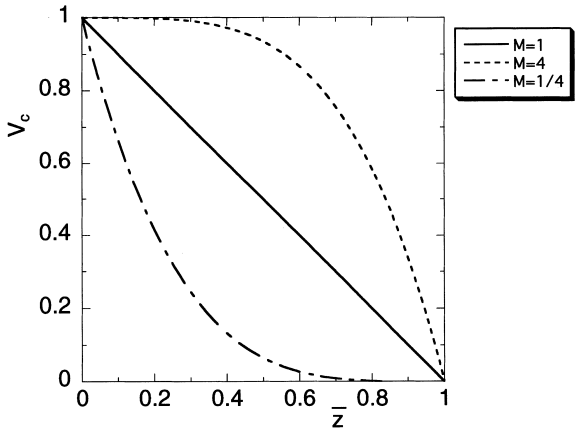

Fig. 2. Variation of volume fraction V_c.

In the case of FGM plate, substituting Eqs. (20), (56) and the second term of right-hand side of Eq. (39) into Eq. (34), and later comparing the coefficients of functions with regard to $\bar{z}_i$ respectively, the six groups of simultaneous linear equations for $(A_{1ikl}, B_{1ikl}, C_{2ikl})$, $(A_{2ikl}, B_{2ikl}, C_{1ikl})$, $(A^{(j)}_{3ikl}, B^{(j)}_{3ikl}, C^{(j)}_{4ikl})$, $(A^{(j)}_{4ikl}, B^{(j)}_{4ikl}, C^{(j)}_{3ikl})$, $(A^{(j)}_{5ikl}, B^{(j)}_{5ikl}, C^{(j)}_{6ikl})$ and $(A^{(j)}_{6ikl}, B^{(j)}_{6ikl}, C^{(j)}_{5ikl})$ are obtained. Solving these six groups of simultaneous linear equations, the constants $A_{1ikl}, A_{2ikl}, \ldots, C^{(j)}_{5ikl}$, and $C^{(j)}_{6ikl}$ $(i = 1, \ldots, n)$ can be obtained. And, in the case of the piezoelectric plate, substituting Eqs. (20), (56) and the second term of right-hand side of Eq. (39) into Eq. (35), and later comparing the coefficients of functions with regard to $\bar{z}_i$, respectively, the six groups of simultaneous linear equations for $(A_{1ikl}, B_{1ikl}, C_{2ikl}, D_{2kl})$, $(A_{2ikl}, B_{2ikl}, C_{1ikl}, D_{1kl})$, $(A^{(j)}_{3ikl}, B^{(j)}_{3ikl}, C^{(j)}_{4ikl}, D^{(j)}_{4kl})$, $(A^{(j)}_{4ikl}, B^{(j)}_{4ikl}, C^{(j)}_{3ikl}, D^{(j)}_{3kl})$, $(A^{(j)}_{5ikl}, B^{(j)}_{5ikl}, C^{(j)}_{6ikl}, D^{(j)}_{6kl})$ and $(A^{(j)}_{6ikl}, B^{(j)}_{6ikl}, C^{(j)}_{5ikl}, D^{(j)}_{5kl})$ are obtained. Solving these six groups of simultaneous linear equations, the constants A_{1ikl}, $A_{2ikl}, \ldots, C^{(j)}_{5ikl}$, $C^{(j)}_{6ikl}$ $(i = n+1)$, D_{1kl}, D_{2kl}, $D^{(j)}_{3kl}$, $D^{(j)}_{4kl}$, $D^{(j)}_{5kl}$ and $D^{(j)}_{6kl}$ can be obtained. Then, in the case of FGM plate, the stress components can be evaluated by substituting Eq. (39) into Eq. (32), and later into Eq. (27). In the case of the piezoelectric plate, the stress components and the electric displacements can be evaluated by substituting Eq. (39) into Eqs. (30) and (32), and later into Eqs. (28) and (29).

Then the unknown constants in Eqs. (40), (48) and (54) are determined so as to satisfy the boundary conditions (36) and (37).

5. Numerical results

As there are many cases like the thermal, elastic and electric constants for crystal class mm2 don't become clear in the literature, we consider the piezoelectric material of a cadmium selenide solid exhibiting crystal class 6mm which is quoted at the papers of Ashida et al. (1996, 1997). Furthermore, we consider the FGM composed of zirconium oxide (ZrO_2) and titanium alloy (Ti–6Al–4V) which is anticipated as a high-temperature-resistant structural material for thermal stress relaxation in the field of aerospace. It is assumed that the volume fractions of the ceramic phase V_c and the metal phase V_m are given by the relations

$$V_c(\bar{z}) = \left\{ \begin{matrix} 1 - \bar{z}^M; & M \geq 1 \\ (1-\bar{z})^{1/M}; & M \leq 1 \end{matrix} \right\}, \qquad V_m(\bar{z}) = 1 - V_c(\bar{z}); \quad 0 \leq \bar{z} \leq 1 \tag{57}$$

where M is a parameter. And, numerical results are presented for the following values.

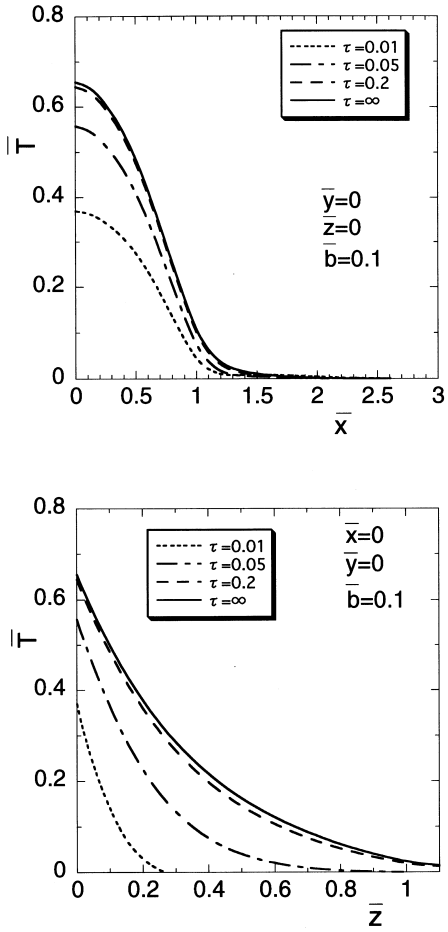

Fig. 3. Temperature change for parameter $M = 1$. (a) variation on the x-axis ($\bar{y} = 0, \bar{z} = 0$), (b) variation in the thickness direction ($\bar{x} = 0, \bar{y} = 0$).

$$H_a = H_b = 5.0, \quad \bar{T}_a = 1.0, \quad \bar{L}_x = \bar{L}_y = 3.0, \quad \bar{b} = 0.1, 0.2, 0.3$$

$$f_a(\bar{x}) = \left(1 - \bar{x}^2/\bar{x}_0^2\right)H(\bar{x}_0 - |\bar{x}|), \qquad g_a(\bar{y}) = \left(1 - \bar{y}^2/\bar{y}_0^2\right)H\left(\bar{y}_0 - |\bar{y}|\right)$$

$$\bar{x}_0 = 1.0, \quad \bar{y}_0 = 1.0, \quad M = 1, 1/4, 4 \tag{58}$$

where $H(x)$ is Heaviside's function. The variation of the volume fraction V_c of the ceramic with the parameter M is shown in Fig. 2. The material constants for zirconium oxide are taken as,

$$\lambda_t = 1.78\ \text{W/mK}, \quad \kappa = 1.06 \times 10^{-6}\ \text{m}^2/\text{s}, \quad \alpha = 8.7 \times 10^{-6}\ 1/\text{K}, \quad Y = 116.4\ \text{GPa}, \quad \nu = 0.33 \tag{59}$$

for titanium alloy,

$$\lambda_t = 6.2\ \text{W/mK}, \quad \kappa = 2.61 \times 10^{-6}\ \text{m}^2/\text{s}, \quad \alpha = 8.9 \times 10^{-6} 1/\text{K}, \quad Y = 105.8\ \text{GPa}, \quad \nu = 0.3 \tag{60}$$

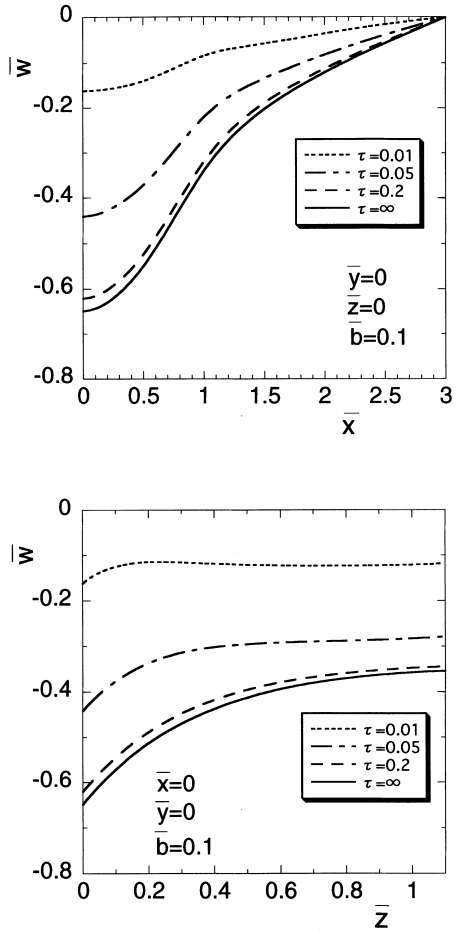

Fig. 4. Thermal displacement $\bar{w}$ for parameter $M = 1$. (a) variation on the x-axis ($\bar{y} = 0, \bar{z} = 0$), (b) variation in the thickness direction ($\bar{x} = 0, \bar{y} = 0$).

and for cadmium selenide (Ashida et al., 1997),

$$\alpha_x = \alpha_y = 4.396 \times 10^{-6}\ 1/\mathrm{K}, \quad \alpha_z = 2.458 \times 10^{-6}\ 1/\mathrm{K}, \quad C_{11} = C_{22} = 74.1\ \mathrm{GPa}$$

$$C_{12} = 45.2\ \mathrm{GPa}, \quad C_{13} = C_{23} = 39.3\ \mathrm{GPa}, \quad C_{33} = 83.6\ \mathrm{GPa}, \quad C_{44} = C_{55} = 13.17\ \mathrm{GPa}$$

$$C_{66} = 14.45\ \mathrm{GPa}, \quad e_{31} = e_{32} = -0.16\ \mathrm{C/m^2}, \quad e_{33} = 0.347\ \mathrm{C/m^2},$$

$$e_{15} = e_{24} = -0.138\ \mathrm{C/m^2}, \quad \eta_{11} = \eta_{22} = 8.25 \times 10^{-11}\ \mathrm{C^2}/Nm^2, \eta_{33} = 9.03 \times 10^{-11}\ \mathrm{C^2/Nm^2}$$

$$p_z = -2.94 \times 10^{-6}\ \mathrm{C/m^2K}, \quad d_1 = -3.92 \times 10^{-12}\ \mathrm{C/N}$$

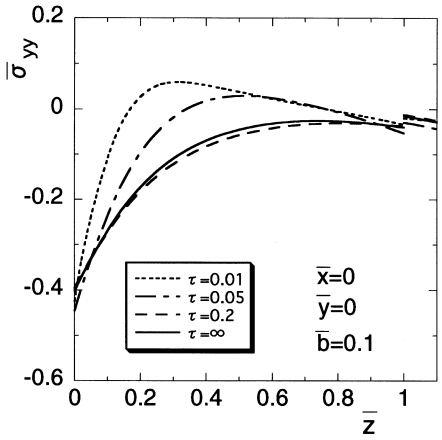

Fig. 5. Variation of the thermal stress $\bar{\sigma}_{yy}$ for parameter $M = 1$ ($\bar{x} = 0, \bar{y} = 0$).

$$\lambda_{tx} = \lambda_{ty} = 8.6\ \mathrm{W/mK}, \quad \lambda_{tz} = 1.5\lambda_{tx} \tag{61}$$

Since the coefficients of thermal conductivity for cadmium selenide could not be found in the literature, the following values are assumed:

$$\kappa_x = \kappa_y = 3.28 \times 10^{-6}\ \mathrm{m^2/s}, \qquad \kappa_z = 1.5\kappa_x \tag{62}$$

The typical values of material properties such as κ_0, λ_{t0}, α_0 and Y_0 used to normalize the numerical data, are based on those of zirconium oxide. To estimate the material properties of FGM, we applied mainly the law of mixture proposed by Kerner (1956a, 1956b), which was derived based on the assumption that there is a granular phase embedded in a matrix phase. However, the details of expression for the law are omitted here for brevity. For numerical calculation, we take $n = 10$ as the number of hypothetical layers in the FGM plate.

Figs. 3–9 show the numerical results for $M = 1$ and $\bar{b} = 0.1$.The variations of temperature change and thermal displacement $\bar{w}$ on the x-axis ($\bar{y} = 0, \bar{z} = 0$) are shown in Figs. 3(a) and 4(a). The variations of

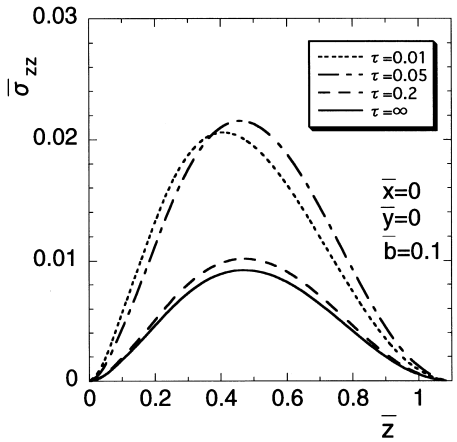

Fig. 6. Variation of the thermal stress$\bar{\sigma}_{zz}$ for parameter $M = 1$ ($\bar{x} = 0, \bar{y} = 0$).

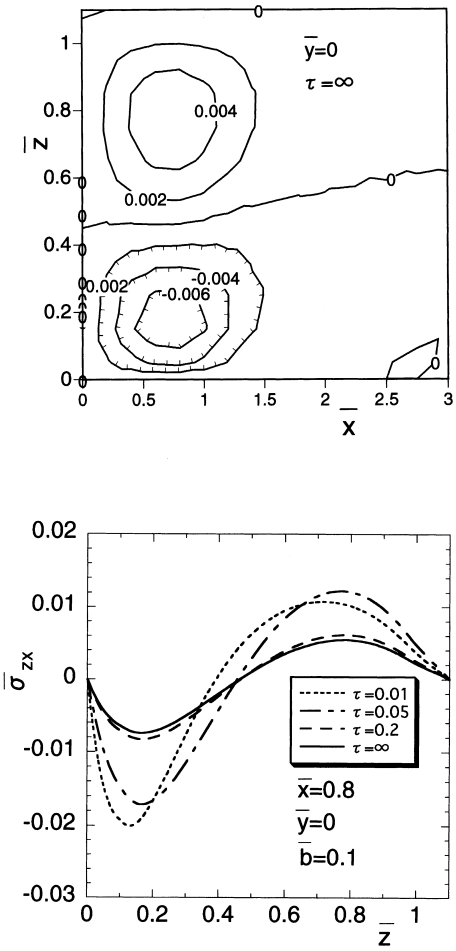

Fig. 7. Thermal stress $\bar{\sigma}_{zx}$ for parameter $M = 1$. (a) distribution in a steady state ($\bar{y} = 0, \tau = \infty$), (b) variation in the thickness direction ($\bar{x} = 0.8, \bar{y} = 0$).

the thickness direction of temperature change and thermal displacement $\bar{w}$ at the midpoint of the plate are shown in Figs. 3(b) and 4(b). As shown in Fig. 3, the temperature rises as the time proceeds and is maximum in the steady state, and the temperature rise can clearly be seen in the heated region. As shown in Fig. 4, the absolute value of thermal displacement $\bar{w}$ rises as the time proceeds and shows the maximum value in the steady state. Fig. 5 and Fig. 6 show the variations of the normal stress $\bar{\sigma}_{yy}$ and $\bar{\sigma}_{zz}$ at the midpoint of the plate, respectively. As shown in Fig. 5, it can be seen that discontinuity occurs on the interface between FGM plate and piezoelectric plate. As shown in Fig. 6, it can be seen that the stress variation becomes substantial with the progress of time and maximum tensile stress occurs in a transient state. Fig. 7 shows the distribution of the shearing stress $\bar{\sigma}_{zx}$. The distribution on the cross-section of $\bar{y} = 0$ in the steady state is shown in Fig. 7(a) and the variation on the cross section ($\bar{x} = 0.8, \bar{y} = 0$) in a transient state is shown in Fig. 7(b). Fig. 7(a) shows that the maximum stress occurs near $\bar{x} = 0.8$ inside of plate. From Fig. 7(b), it can be seen that the shearing stress $\bar{\sigma}_{zx}$ shows the

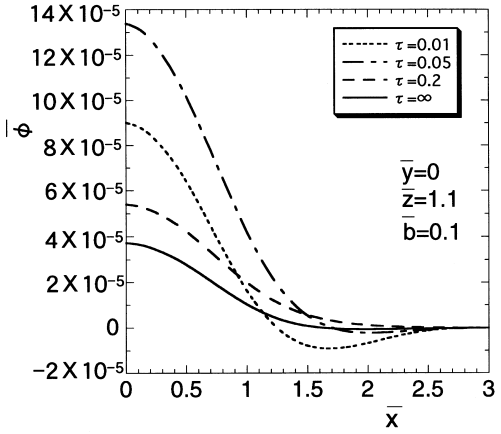

Fig. 8. Variation of the electric potential for parameter $M = 1$.

maximum value at $z \cong 0.15$ in a transient state. Figs. 8 and 9 show the variations of the electric potential and the electric displacement $\bar{D}_x$ on the top surface ($\bar{y} = 0, \bar{z} = 1.1$), respectively. From Figs. 8 and 9, it can be seen that the variations become substantial with the progress of time and maximum value occurs in a transient state.

In order to examine the influence of the parameter M of the material composition, the variations of temperature change, thermal stress $\bar{\sigma}_{zz}$, thermal stress $\bar{\sigma}_{zx}$, and electric potential for $\bar{b} = 0.1$ are shown in Figs. 10–13, respectively. From Fig. 10, it can be seen that the temperature change on the heated side of the plate is decreased when the parameter M reduces. As shown in Figs. 11 and 12, it can be seen that the maximum values of the normal stress $\bar{\sigma}_{zz}$ and shearing stress $\bar{\sigma}_{zx}$ and their distributions are substantially changed when the parameter M is changed. Then, it can be seen from Fig. 13 that the maximum values of the electric potential are decreased when the parameter M reduces.

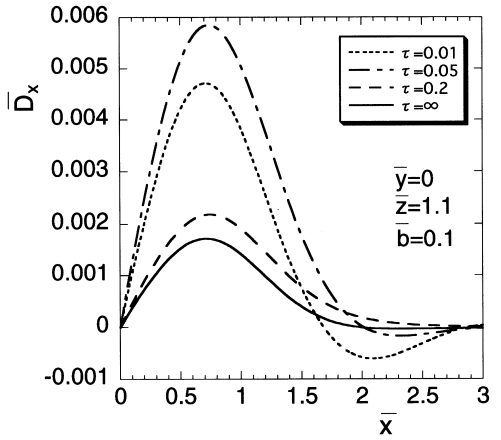

Fig. 9. Variation of the electric displacement $\bar{D}_x$ for parameter $M = 1$.

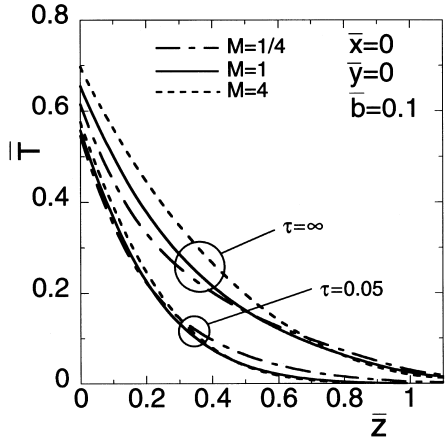

Fig. 10. Influence of parameter M on temperature change ($\bar{x} = 0, \bar{y} = 0$).

Fig. 14 shows the influence of thickness $\bar{b}$ of piezoelectric plate on electric potential on the top surface ($\bar{y} = 0, \bar{z} = 1 + \bar{b}$). Then, it can be seen from Fig. 14 that the value of the electric potential is increased when the thickness $\bar{b}$ increases.

Finally, in order to assess the influence of the functional grading, the numerical results for the homogeneous plate composed of zirconium oxide and the piezoelectric plate composed of a cadmium selenide solid for $\bar{b} = 0.1$ are shown in Fig. 15. The variations of the thickness direction of temperature change and normal stress $\bar{\sigma}_{zz}$ at the midpoint of the plate are shown in Fig. 15(a) and (b), respectively. The variation of shearing stress $\bar{\sigma}_{zx}$ on the cross section ($\bar{x} = 0.8, \bar{y} = 0$) is shown in Fig. 15(c). From Figs. 11, 12, 15(a) and (c), it is possible to decrease the maximum values of normal stress $\bar{\sigma}_{zz}$ and shearing stress $\bar{\sigma}_{zx}$ in a transient state by the functional grading.

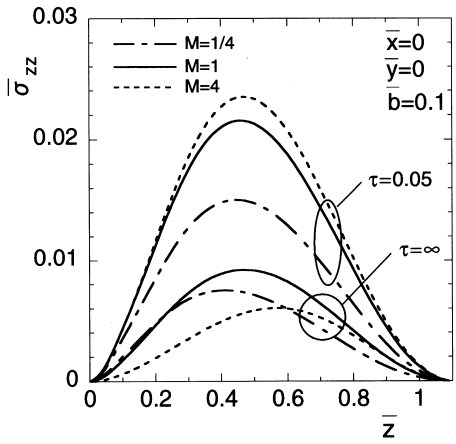

Fig. 11. Influence of parameter M on thermal stress $\bar{\sigma}_{zz}$ ($\bar{x} = 0, \bar{y} = 0$).

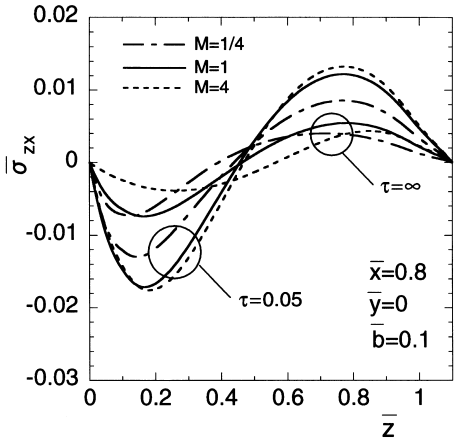

Fig. 12. Influence of parameter M on thermal stress $\bar{\sigma}_{zx}$ ($\bar{x} = 0.8, \bar{y} = 0$).

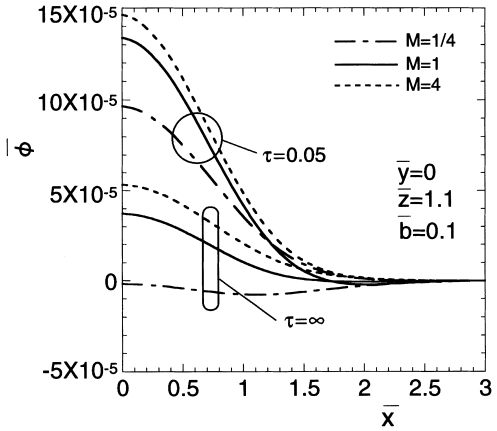

Fig. 13. Influence of parameter M on electric potential.

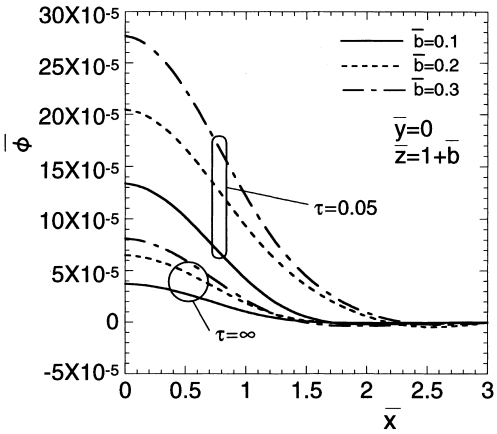

Fig. 14. Influence of thickness $\bar{b}$ of piezoelectric plate on electric potential.

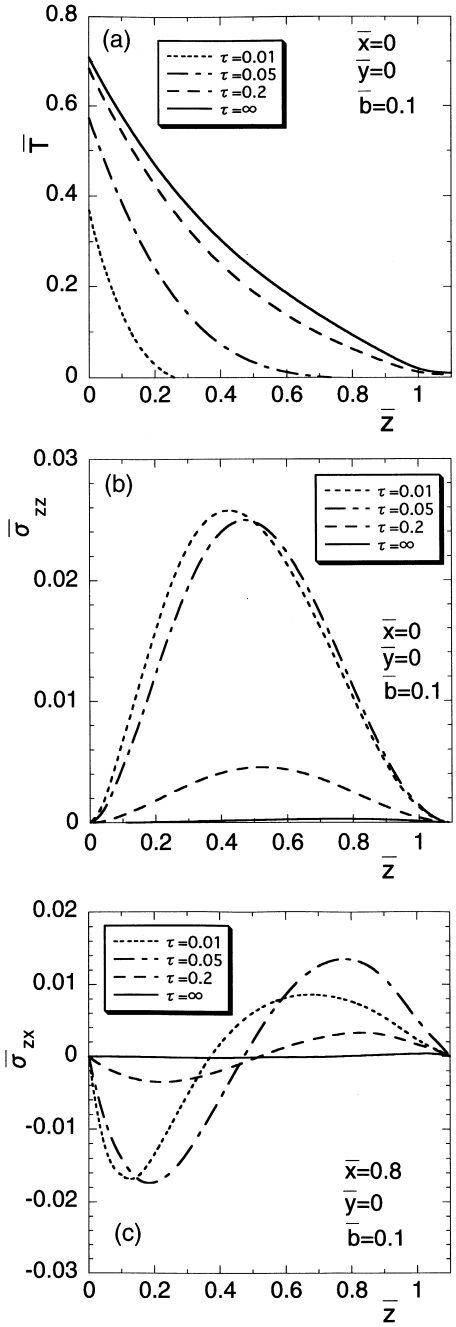

Fig. 15. Results for combined plate composed of homogeneous material and piezoelectric material. (a) Temperature change ($\bar{x}=0$, $\bar{y}=0$,), (b) Thermal stress $\bar{\sigma}_{zz}$ ($\bar{x}=0$, $\bar{y}=0$), (c) Thermal stress $\bar{\sigma}_{zx}$ ($\bar{x}=0.8$, $\bar{y}=0$).

6. Conclusions

In this study, we analyzed the three-dimensional transient piezothermoelasticity problem involving a functionally graded rectangular plate bonded to a piezoelectric plate of crystal class mm2 due to partial heat supply. As an illustration, we carried out numerical calculations for the functionally graded plate composed of zirconium oxide and titanium alloy, bonded to a piezoelectric plate of a cadmium selenide solid and examined the behaviors in the transient state for the temperature change, the displacement, the stress, electric potential, and electric displacement distributions. We conclude that we can evaluate not only all stresses of the combined plate but also the electric field of the piezoelectric plate quantitatively in a transient state.

Appendix A

$$
\begin{aligned}
f_{11} &= A_{12}\left(\bar{C}_{33}\bar{\eta}_{33} + \bar{e}_{33}^2\right) - A_{13}\left(A_{23}\bar{\eta}_{33} + A_{24}\bar{e}_{33}\right) + A_{14}\left(A_{24}\bar{C}_{33} - A_{23}\bar{e}_{33}\right)\\
f_{12} &= -A_{12}\left(A_{33}\bar{\eta}_{33} - \bar{C}_{33}A_{44} + 2A_{34}\bar{e}_{33}\right) - A_{13}(A_{23}A_{44} - A_{24}A_{34}) + A_{14}(A_{23}A_{34} - A_{24}A_{33})\\
f_{13} &= -A_{12}\left(A_{33}A_{44} - A_{34}^2\right)\\
f_{21} &= -A_{13}\bar{C}_{44}\bar{\eta}_{33} - A_{14}\bar{C}_{44}\bar{e}_{33}\\
f_{22} &= A_{13}\left(A_{22}\bar{\eta}_{33} - A_{44}\bar{C}_{44} + A_{24}^2\right) - A_{12}\left(A_{23}\bar{\eta}_{33} + A_{24}\bar{e}_{33}\right) + A_{14}\left(A_{22}\bar{e}_{33} + A_{34}\bar{C}_{44} - A_{23}A_{24}\right)\\
f_{23} &= -A_{12}(A_{23}A_{44} - A_{24}A_{34}) - A_{22}A_{34}A_{14} + A_{22}A_{44}A_{13}\\
f_{31} &= -A_{13}\bar{C}_{44}\bar{e}_{33} + A_{14}\bar{C}_{44}\bar{C}_{33}\\
f_{32} &= A_{13}\left(A_{22}\bar{e}_{33} + \bar{C}_{44}A_{34} - A_{23}A_{24}\right) + A_{12}\left(A_{24}\bar{C}_{33} - A_{23}\bar{e}_{33}\right) + A_{14}\left(A_{23}^2 - A_{22}\bar{C}_{33} - A_{33}\bar{C}_{44}\right)\\
f_{33} &= A_{12}(A_{23}A_{34} - A_{24}A_{33}) + A_{14}A_{22}A_{33} - A_{13}A_{22}A_{34}
\end{aligned}
\tag{A1}
$$

$$
\begin{aligned}
g_1 &= \bar{C}_{44}\bar{e}_{33}^2 + \bar{C}_{33}\bar{C}_{44}\bar{\eta}_{33}\\
g_2 &= \bar{\eta}_{33}\left(A_{23}^2 - A_{33}\bar{C}_{44} - A_{22}\bar{C}_{33}\right) - A_{22}\bar{e}_{33}^2 + 2\bar{e}_{33}\left(A_{23}A_{24} - A_{34}\bar{C}_{44}\right) + A_{44}\bar{C}_{44}\bar{C}_{33} - A_{24}^2\bar{C}_{33}\\
g_3 &= A_{22}\left(A_{33}\bar{\eta}_{33} - A_{44}\bar{C}_{33} + 2A_{34}\bar{e}_{33}\right) - 2A_{23}A_{24}A_{34} + A_{44}\left(A_{23}^2 - \bar{C}_{44}A_{33}\right) + A_{24}^2A_{33} + A_{34}^2\bar{C}_{44}\\
g_4 &= A_{22}\left(A_{33}A_{44} - A_{34}^2\right)
\end{aligned}
\tag{A2}
$$

References

Ashida, F., Choi, J.S., Noda, N., 1996. An inverse thermoelastic problem in an isotropic plate associated with a piezoelectric ceramic plate. J. Thermal Stresses 19, 153–167.

Ashida, F., Choi, J.S., Noda, N., 1997. Control of elastic displacement in piezoelectric-based intelligent plate subjected to thermal load. Int. J. Engng. Sci 35, 851–868.

Choi, J.S., Ashida, F., Noda, N., 1997. Control of thermally induced elastic displacement of an isotropic structural plate bonded to a piezoelectric ceramic plate. Acta Mech 122, 49–63.

Heyliger, P., 1997. Exact solutions for simply supported laminated piezoelectric plates. ASME J. Appl. Mech 64, 299–306.

Kerner, E.H., 1956a. The electrical conductivity of composite media. Proc. Phys. Soc. Lond 69B, 802–807.

Kerner, E.H., 1956b. The elastic and thermo-elastic properties of composite media. Proc. Phys. Soc. Lond 69B, 808–813.

Noda, N., Kimura, S., 1998. Deformation of a piezothermoelectric composite plate considering the coupling effect. J. Thermal Stresses 21, 359–379.

Obata, Y., Noda, N., 1993. Transient thermal stresses in a plate of functionally gradient material. Ceramic Trans 34, 403–410.

Ootao, Y., Akai, T., Tanigawa, Y., 1995a. Three-dimensional transient thermal stress analysis of a nonhomogeneous hollow circular cylinder due to a moving heat source in the axial direction. J. Thermal Stresses 18, 497–512.

Ootao, Y., Tanigawa, Y., 1995b. Three-dimensional transient thermal stress analysis of a nonhomogeneous hollow sphere due to rotating heat source. In: Proceedings of the First International Symposium on Thermal Stresses and Related Topics, Hamamatsu, 339–342.

Pagano, N.J., 1970. Exact solutions for rectangular bidirectional composites and sandwich plates. J. Composite Materials 4, 20–34.

Qiu, J., Tani, J., Takagi, T., 1994. An intelligent piezoelectric composite material without bending deformation. J. Rech. Phys 35, 99–107.

Rao, S.S., Sunar, M., 1994. Piezoelectricity and its use in disturbance sensing and control of flexible structures: a survey. Appl. Mech. Rev 47, 113–123.

Sugano, Y., 1987. An expression for transient thermal stress in a nonhomogeneous plate with temperature variation through thickness. Ing. Arch 57, 147–156.

Tanigawa, Y., Akai, T., Kawamura, R., Oka, N., 1996. Transient heat conduction and thermal stress problems of a nonhomogeneous plate with temperature-dependent material properties. J. Thermal Stresses 19, 77–102.

Tauchert, T.R., 1992. Piezothermoelastic behavior of a laminated plate. J. Thermal Stresses 15, 25–37.